ARTICLE NO. 78-1083

Effect of Over-the-Wing Nacelles on Wing-Body Aerodynamics

David E. Reubush*
NASA Langley Research Center, Hampton, Va.

An investigation was conducted in the Langley 16-ft transonic tunnel to further study benefits in climb and cruise performance due to blowing the jet over the wing for a transport-type wing-body configuration. In this investigation, a wing-body model powered-nacelle test rig combination was tested at Mach numbers of 0.5 and 0.8 at angles of attack from −2-4 deg and jet total-pressure ratios from jet off to 3 or 4 (depending on Mach number) for a variety of nacelle locations relative to the wing. Results from this investigation show that positioning of the nacelles can have very large effects on the wing-body drag (nacelles were nonmetric). Some positions yielded much higher drag than the baseline wing-body, while others yielded drag somewhat lower than the baseline.

Nomenclature

C_D = drag coefficient
C_L = lift coefficient
C_m = pitching moment coefficient
D = jet-exit diameter
JO = jet off
LE = leading edge
M = Mach number
NPR = nozzle pressure ratio—ratio of jet total-pressure to freestream static pressure
x = position of nacelle exit with respect to wing leading edge-positive aft
W-B = wing-body
wrt = with respect to
z = height of centerline of nacelle exit above wing chord plane
α = angle of attack

Introduction

NASA currently has an agressive program underway to develop technology that will enable the next generation of transport aircraft to be designed with improved performance, reduced fuel consumption, and reduced environmental impact. In this program, a number of unconventional engine placements have been investigated. One of the most promising configurations appears to be the over-the-wing (OTW) arrangement in which the engine nacelles are supported on pylons above the wing upper surface. Falk,[1] a German researcher, first investigated the effects of blowing a jet over a wing during World War II while doing research to determine the effect of jet exhaust on tail surfaces. However, it was not until the early 1970s that this type of configuration was looked at again,[2,3] primarily due to the expected gain in noise reduction resulting from the shielding of the jet exhaust by the wing. At this point it was realized that, in addition to the anticipated benefits in noise reduction, this type of configuration arrangement resulted in increased lift and reduced induced drag. As a result of these performance gains, the VFW-614 was designed and built with over-the-wing nacelles.[3] More recently, Mercer and Carson[4] and Coe, et al.[5] at NASA Langley investigated this type of arrangement applied to SST configurations.

Although the VFW-614 is flying with over-the-wing nacelles and there have been data published for supersonic transport configurations with over-the-wing nacelles, there is a scarcity of published data for subsonic transport configurations. This lack of experimental data has hindered the verification of the various theoretical techniques[6-10] which have been developed to predict the performance gains from this type of engine arrangement. In an effort to partially alleviate this problem and gain further insight into the mechanisms involved, an experimental investigation was initiated at NASA Langley. In this investigation the movable nacelle support mechanism first used in the investigation of Ref. 4 was modified to incorporate nacelles the size of typical high bypass ratio turbofan nacelles. Using this mechanism, an existing wing-body model typical of a subsonic transport configuration was tested with the nacelles positioned over the wing in several locations. The results of this investigation were reported in Ref. 11. Unfortunately, interference from the supporting/translating mechanism for the nacelles invalidated the measured total drag data, and only induced drag data were presented. These data, however, showed that the induced drag for most over-the-wing nacelle configurations tested was lower than that for the basic wing-body. As a result of these promising results, a new investigation was initiated. In this investigation, the boattailed aft fuselage of the model of Ref. 11 was replaced by a cylindrical aft fuselage with extensive base pressure instrumentation. The revised model was tested at Mach numbers of 0.5 and 0.8 at angles of attack of −2-4 deg with jet total-pressure ratios from jet off to a maximum of 4, depending on Mach number. Positions of the nacelles relative to the wing were chosen based on the data of Ref. 11. The purpose of this paper is to discuss the results of this investigation.

Experimental Methods

The wing-body model with nacelles and nacelle supporting/translating apparatus mounted in the Langley 16-ft transonic tunnel is shown in Fig. 1. The body of the model was 124.0 cm long and had a maximum diameter of 12.5 cm. The wing was swept back 35 deg at the quarter-chord, had an aspect ratio of 6, an NACA 63A008 airfoil section, a span of 91.4 cm, a root chord of 21.77 cm, a tip chord of 8.71 cm, and a mean geometric chord of 15.24 cm. The two nacelles each were 44.5 cm long, had a maximum diameter of 7.1 cm, and a jet exit diameter of 5.1 cm. The wing-body model was mounted on a six-component strain-gage balance which was used to measure the forces and moments. The nacelles and supporting apparatus were nonmetric.

Tests were conducted at Mach numbers of 0.5 and 0.8, at angles of attack from −2-4 deg, with nozzle total-pressure ratios from jet off to 3 at $M=0.5$ and jet off to 4 at $M=0.8$. Transition was applied to the nose and wings of the model according to the methods of Refs. 12 and 13 to insure tur-

Presented as Paper 78-1083 at the AIAA/SAE 14th Joint Propulsion Conference, Las Vegas, Nev., July 25-27, 1978; submitted Aug. 18, 1978; revision received Dec. 20, 1978.

Index categories: Aerodynamics; Airbreathing Propulsion.

*Aerospace Engineer, Propulsion Aerodynamics Branch, High-Speed Aerodynamics Division. Member AIAA.

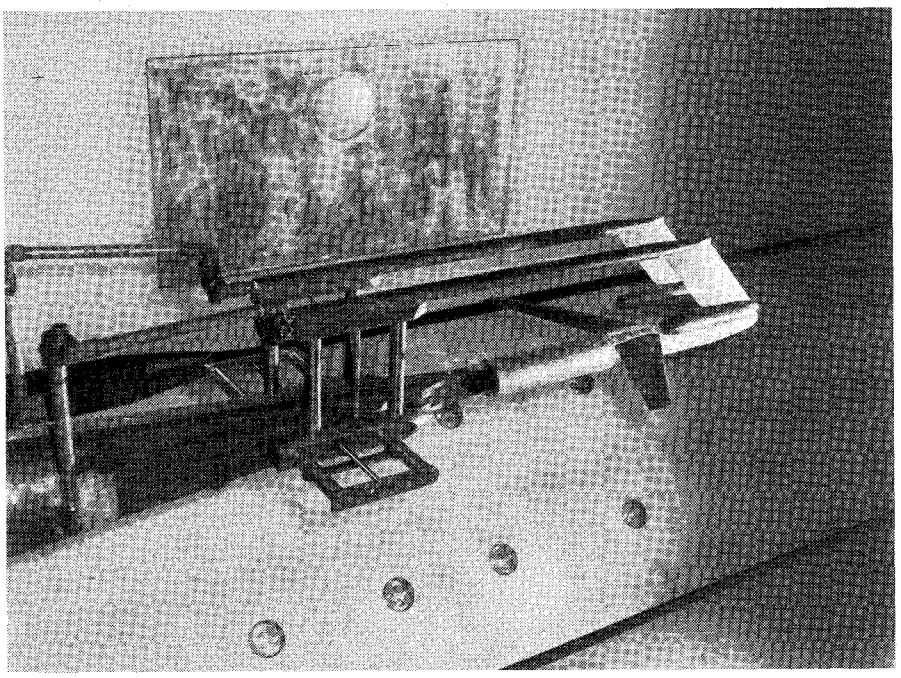

Fig. 1 Wing-body model with nacelles and support apparatus installed in Langley 16-ft transonic tunnel.

Table 1 Test matrix

	25% semispan			50% semispan
x/D \ z/D	0.5	1.0	1.5	1.0
−1		x		
0	x	x	x	x
1		x		x
1½		x		
2		x		
3		x		

bulent flow at all test conditions. The nacelle support apparatus allowed three degrees of translational freedom in locating the nacelles relative to the wing. With this capability available, the wing-body was tested with the centerline of the nacelle exits in a variety of locations, as shown in Table 1. At the 25% semispan station, the wing chord was 18.50 cm, while at the 50% semispan station, the wing chord was 15.24 cm. These dimensions are provided to facilitate conversion of positions in terms of nacelle exit diameters to positions in terms of local chord.

Results

As mentioned previously, only induced drag coefficients were presented in Ref. 11, due to an interference effect from the nacelle supporting/translating apparatus which affected the boattailed aft fuselage of the model. In the current investigation, the boattailed aft fuselage of Ref. 11 was replaced by a cylindrical aft fuselage with extensive base pressure instrumentation. With this type of fuselage, the interference should be limited to changes in the base pressures. It should, therefore, be possible to eliminate the interference effect on the model drag by correcting for changes in these base pressures. To assess the effect of the nacelle support system, the nacelles, nacelle support booms, and pylons were removed leaving only the aft supporting/translating mechanisms, and tests were made with these supports in the locations corresponding to the locations for the various nacelle positions (a total of 10). The range of drag coefficient data obtained is shown in Fig. 2 at both $M=0.5$ and 0.8. As can be

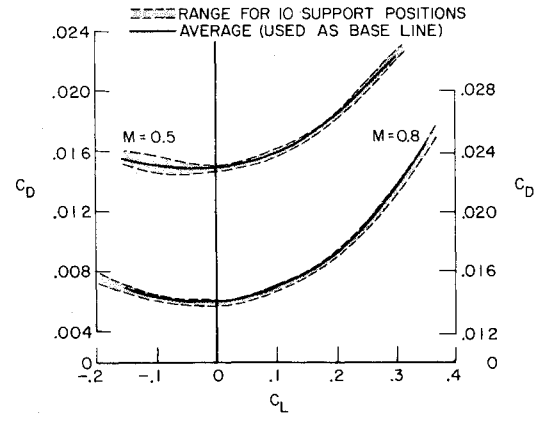

Fig. 2 Effect of aft support movement on baseline wing-body drag.

seen, the drag coefficients do not vary significantly at either Mach number. The drag remains well within the band of experimental accuracy at both $M=0.5$ and 0.8. These results indicate that movement of this supporting/translating apparatus has only a small effect, if any, on model drag after it has been corrected for base drag. Therefore, the average drag coefficient curves (both $M=0.5$ and 0.8) for the ten runs are plotted as solid lines on Fig. 2, and these curves will be used as the baseline for comparison purposes in succeeding figures. The baseline curves for lift, drag, and pitching moment in succeeding figures will appear as shaded curves of finite width in order to facilitate differentiation from the data with which they are being compared.

Effect of NPR

Wing-body drag coefficient curves for a typical configuration (nacelle exits 1D above the wing, 1D aft of the leading edge, and 25% semispan) at the various nozzle pressure ratios (NPRs) investigated at both $M=0.5$ and 0.8 are shown in Fig. 3. For the range of pressure ratios investigated, the largest change in drag coefficient (a large increase especially near $C_L=0.1$) occurs when the jet is first turned on with only relatively small changes as the pressure ratio is increased. These data indicate the presence of the

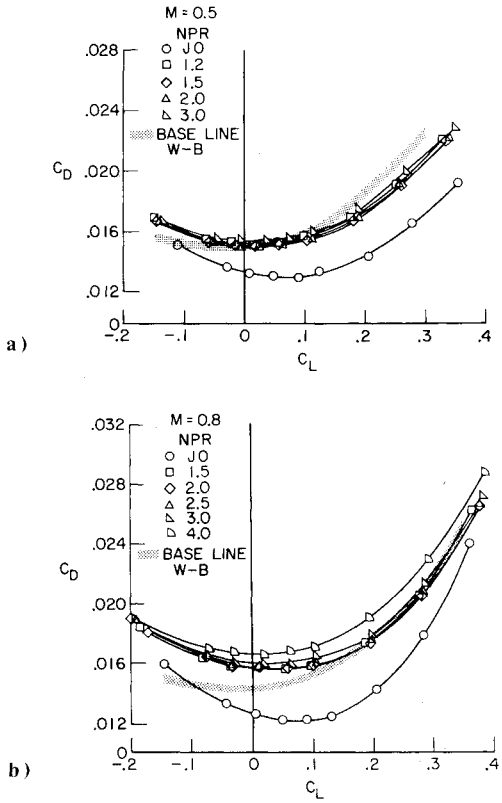

Fig. 3 Effect of NPR on wing-body drag. Nacelle exits: $x/D = 1$, $y/(b/2) = 0.25$, $z/D = 1$. a) $M = 0.5$; b) $M = 0.8$.

nacelles has a beneficial interference effect on the wing-body drag, and operation of the jet tends to reduce this beneficial effect. There are two mechanisms to which those effects can be attributed. The solid blockage effect of the presence of the nacelle and the low-energy wake behind it interact with the wing-body and reduce the drag, while the operation of the jet tends to reduce the solid blockage effect and eliminates the low-energy flow behind the nacelle, thereby increasing the drag. Another interesting but smaller effect is seen, especially at $M = 0.8$, in that the drag curves remain essentially the same for jet-on NPRs below 3, while the drag at NPR = 3 is slightly higher, and at NPR = 4 the drag is higher still. It is believed that this phenomenon is an indication that the jet plume has spread sufficiently at these higher NPRs so that it hits the wing yielding a scrubbing drag and possibly a wave drag not found at the lower NPRs. Therefore, care should be exercised in the design of real aircraft configurations to insure that the plume at the engine-operating NPR will not impinge on the wing.

Wing-body lift and pitching moment coefficient characteristics with variations in jet total pressure ratio at $M = 0.8$ for the same typical configuration as in Fig. 3 are shown in Fig. 4. (Lift and pitching moment data are only shown at $M = 0.8$ for this and further comparisons because the results at $M = 0.8$ are typical of both Mach numbers investigated and the effects of any variable on either lift or pitching moment are generally small.) As with drag coefficient, there is a relatively large decrease in pitching moment once the jet has been turned on, and then only very minor changes with increases in NPR. There are only small effects of jet operation on the stability of the configuration, however. The lift curves generally show only very small changes in level with NPR but retain approximately the same slope. These results are encouraging in that there are no large changes in stability which would have to be dealt with for a configuration utilizing this engine arrangement.

Since changes in NPR, once the jet has been turned on, have only small effects on wing-body aerodynamic characteristics, all further comparisons between various nacelle positions will be presented at constant values of NPR. It is anticipated that a typical future high bypass ratio engine will deliver a constant total-pressure rise factor of approximately 1.6 over its subsonic Mach number operating envelope. This total pressure rise factor translates into an NPR of approximately 2.0 at $M = 0.5$ and 2.5 at $M = 0.8$. These, then, are the NPRs at which the comparison data will be presented.

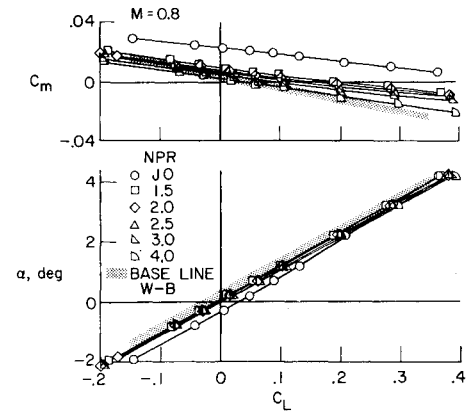

Fig. 4 Effect of NPR on wing-body lift and pitching moment. Nacelle exits: $x/D = 1$, $y/(b/2) = 0.25$, $z/D = 1$.

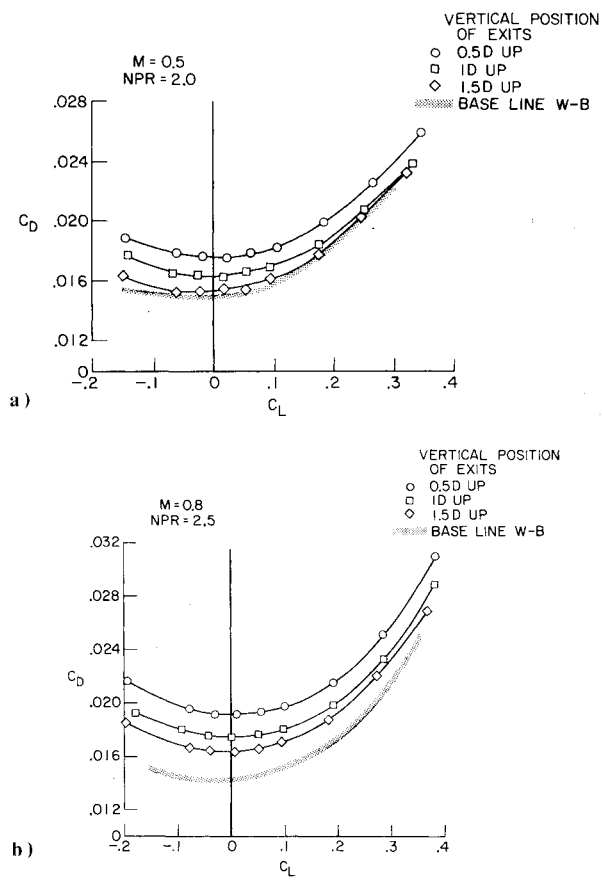

Fig. 5 Effect of nacelle exit vertical location on wing-body drag. Nacelle exits: $x/D = 0$, $y/(b/2) = 0.25$. a) $M = 0.5$, NPR = 2.0; b) $M = 0.8$, NPR = 2.5.

Effect of Nacelle Height

The effect of nacelle-exit vertical location on wing-body drag at the Mach numbers of 0.5 and 0.8 for configurations with the nacelle exits at the leading edge and 25% semispan station is shown in Fig. 5. As would be expected, the configuration with the nacelle exits at ½ diam above the wing (equivalent to upper-surface blowing) has the highest drag

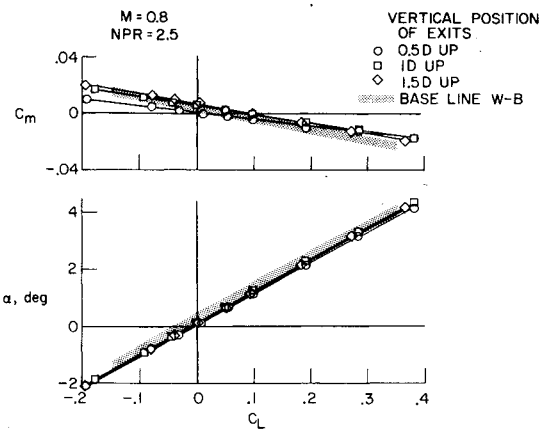

Fig. 6 Effect of nacelle exit vertical location on wing-body lift and pitching moment. Nacelle exits: $x/D=0$, $y/(b/2)=0.25$.

due to the scrubbing drag associated with the jet washing the wing. The two other configurations exhibit progressively lower drag as the nacelles are raised above the wing (at least for the positions tested). The trend with nacelle height, therefore, reveals that as the nacelles are raised above the wing, and hence the jet moves away from the surface of the wing, the drag is reduced. However, in the range of operating C_L around 0.3, the drag of the 1½ diam above the wing configuration is not much lower than the 1 diam above the wing configuration, especially at $M=0.5$. In designing a real configuration, this relatively small benefit would have to be weighed against the increased weight required due to the longer pylon. To be consistent with the work reported in Ref. 11, all of the following comparisons will be made for configurations with the nacelle exits 1 exit-diam above the wing.

The effects of nacelle-exit vertical position on the wing-body lift and pitching moment characteristics at $M=0.8$ are shown in Fig. 6. Increasing nacelle height above the wing causes a small increase in longitudinal stability, while the changes in the lift curve with nacelle height are very minor. Again, there are no large changes in aerodynamic characteristics which would have to be accounted for in a design utilizing this type of engine arrangement.

Effect of Nacelle Span Location

Nacelle-exit span location effect on wing-body drag for the nacelle exits 1 exit-diam above the wing at the leading edge and 1 exit-diam aft of the leading edge at Mach numbers of 0.5 and 0.8 are shown in Figs. 7 and 8. For both leading edge and 1 exit-diam aft of the leading-edge configurations, there are significant reductions in drag to be realized when the nacelles are moved outboard. While these demonstrated reductions in drag hold promise, the problem of one-engine-out controllability will generally preclude use of such an outboard location. It is believed that the benefits seen from the outboard location are due to the beneficial solid blockage interference from the presence of the nacelles being able to propagate further over the wing before interacting with the effect of the body.

At this point, it should be mentioned that at lift coefficients near 0.3, the drag of the configuration with the nacelle exits at the leading edge, 1 exit-diam above the wing at 50% semispan, is lower at both $M=0.5$ and 0.8 than the baseline wing-body configuration. At 1 diam aft of the leading edge, both 25% and 50% semispan configurations have lower drag than the baseline wing-body over almost the whole C_L range, and the 50% semispan configuration has substantially lower drag than the baseline in the range of C_L's for cruise. Having shown in Fig. 3 that jet operation has a detrimental effect on wing-body drag, these improvements in drag over the baseline wing-body must be due to a very large beneficial interference effect on the wing caused by the presence of the nacelles.

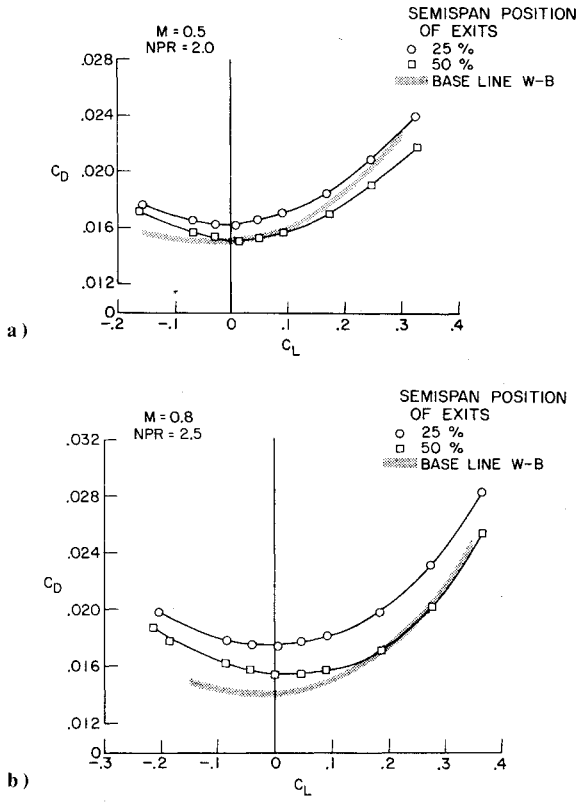

Fig. 7 Effect of nacelle exit span location on wing-body drag. Nacelle exits: $x/D=0$, $z/D=1$. a) $M=0.5$, NPR = 2.0; b) $M=0.8$, NPR = 2.5.

Whether there is a corresponding detrimental effect on the nacelles themselves is unknown, since the nacelles were, of necessity, nonmetric. This question is one which should be answered before any real aircraft designs are proposed with this type of engine arrangement. However, the current data are indeed promising.

While nacelle span location effects on wing-body drag are shown in Figs. 7 and 8, the effects of nacelle span location on lift and pitching moment are shown in Fig. 9 for the 1 exit-diam aft configuration which is typical. Whenever large drag reductions, such as exhibited in Figs. 7 and 8 occur, there is often accompanying concern over whether the improvements shown will disappear when trim drag and other factors are taken into account. Fortunately, the lift and pitching characteristics for these configurations, as well as previously discussed configurations which do not exhibit reductions in drag as significant as these, change only slightly, if at all. The trend in pitching moment coefficient with span location for both leading edge and 1 exit-diam aft of the leading edge configurations, is for the level to be reduced slightly at the 50% semispan station compared to the 25% semispan station, while the slope remains about the same at both positions. The slopes of the pitching moment coefficient curves for all four configurations are somewhat less than that for the wing-body alone. The effect of spanwise movement of the nacelles on wing-body lift coefficient is small at both the leading edge and 1 exit-diam aft of the leading edge. In addition, the lift curves for all four configurations are very close to that of the baseline wing-body.

Effect of Nacelle Longitudinal Location

Figures 10 and 11 present the effect of nacelle exit longitudinal location on wing-body drag at 25% and 50% semispan stations, respectively (nacelle exits 1 exit-diam above the wing). As can be seen from Fig. 10, this position variable was extensively investigated at the 25% semispan station. This extensive investigation was due in part to the

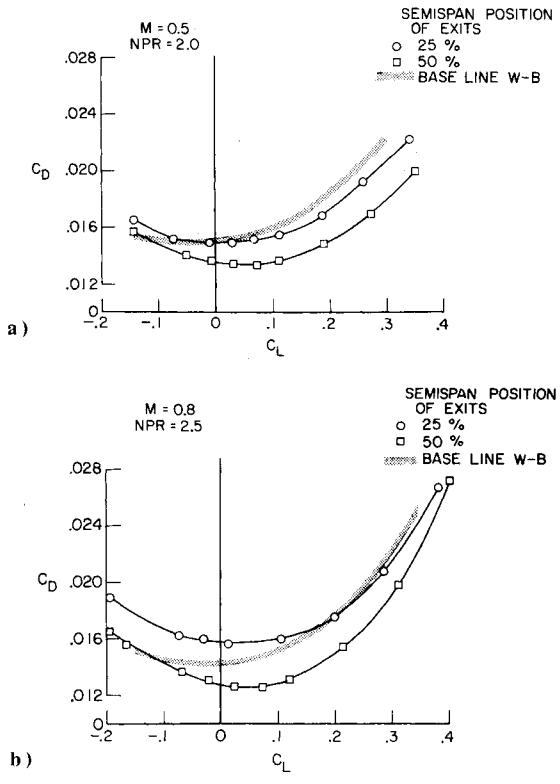

Fig. 8 Effect of nacelle exit span location on wing-body drag. Nacelle exits: $x/D = 1$, $z/D = 1$. a) $M = 0.5$, NPR = 2.0; b) $M = 0.8$, NPR = 2.5.

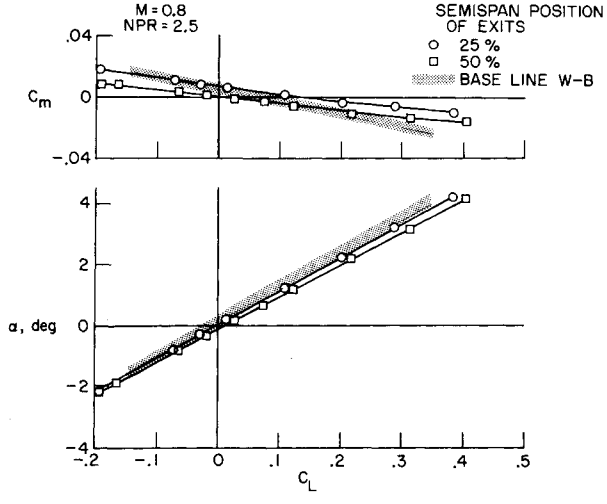

Fig. 9 Effect of nacelle exit span location on wing-body lift and pitching moment. Nacelle exits: $x/D = 1$, $z/D = 1$.

results from the test reported in Ref. 11 which indicated that moving the nacelles aft caused a reduction in induced drag. The current data indicate that as the nacelles are moved aft from 1 exit-diam forward of the leading edge, the drag polars initially tend to rotate, such that the drag coefficient at cruise C_L's (e.g., 0.3) are lower as the nacelles are moved aft. At nacelle exit locations 1 exit-diam or greater aft of the leading edge, the shape of the drag polars begins to change, such that there are cross-overs in relative position with one nacelle exit position having lower drag at some C_Ls and another position at other C_L's. Also, the relative positions of the polars are not exactly the same at both Mach numbers. However, at both $M = 0.5$ and 0.8 and at C_L's above approximately 0.2, the 1½ exit-diam aft of the leading edge configuration has the lowest drag of any of this series. In addition, when the nacelle exits

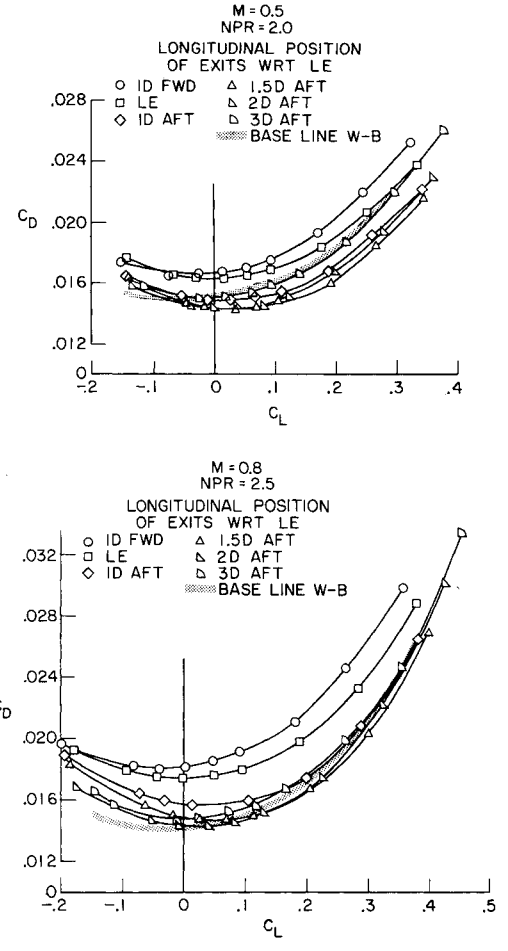

Fig. 10 Effect of nacelle exit longitudinal location on wing-body drag. Nacelle exits: $y/(b/2) = 0.25$, $z/D = 1$. a) $M = 0.5$, NPR = 2.0; b) $M = 0.8$, NPR = 2.5.

are moved from 2 exit-diam aft of the leading edge to 3 exit-diam aft of the leading edge, the general trend of a reduction in drag with aft movement is reversed. The reason for the reversal in trend is not clear at present and needs further study.

At the 50% semispan position (Fig. 11), only two axial nacelle exit locations were investigated: nacelle exits at the leading edge and nacelle exits 1 exit-diam aft of the leading edge. As with the 25% semispan position, the 1 exit-diam aft of the leading-edge configuration has substantially lower drag than the leading-edge configuration at both Mach numbers. Although the optimum axial location at the 50% semispan station was not determined, the 1 exit-diam aft of the leading-edge configuration does have the lowest drag of any of the nacelle exit positions tested, and the drag is substantially below that of the baseline wing-body.

The effects of nacelle exit longitudinal position on wing-body lift and pitching moment for the 25% semispan configuration are shown in Fig. 12 and are typical. At both 25% and 50% semispan stations, there are only minor effects of nacelle longitudinal location on wing-body pitching moment coefficient with the exception of the configuration with the nacelle exits 3 exit-diam aft of the leading-edge at 25% semispan. For this configuration, there is a reduction in level of the pitching moment curve over that for the other configurations. The underlying causes for this shift are probably the same as those that caused the reversal of the drag coefficient trend with this configuration and, as such, have not been fully identified. Aft movement of the nacelles caused a small change in lift at zero angle of attack without changing the lift-curve slope for all configurations at both 25% and 50% semispan stations.

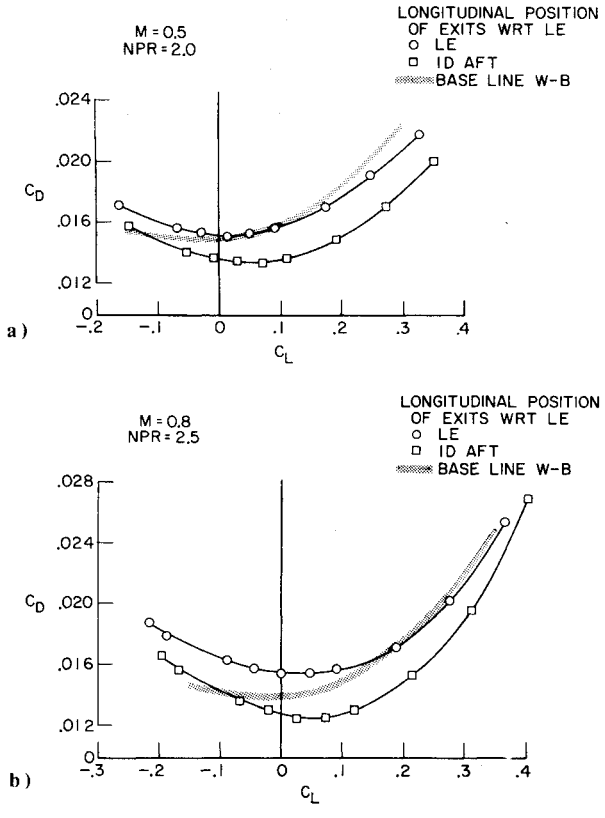

Fig. 11 Effect of nacelle exit longitudinal location on wing-body drag. Nacelle exits: $y/(b/2) = 0.50$, $z/D = 1$. a) $M = 0.5$, NPR = 2.0; b) $M = 0.8$, NPR = 2.5.

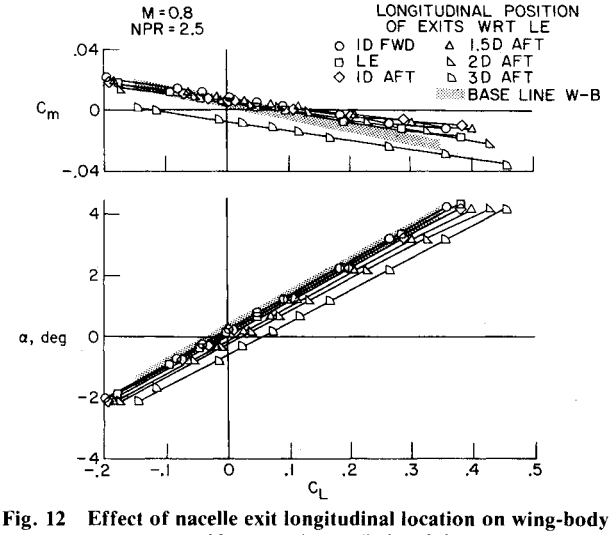

Fig. 12 Effect of nacelle exit longitudinal location on wing-body lift and pitching moment. Nacelle exits: $y/(b/2) = 0.25$, $z/D = 1$.

Summary of Results

Summary plots of the trends in wing-body drag with nacelle position at a typical cruise C_L of 0.3 for both $M = 0.5$ and 0.8 are shown in Fig. 13. The first part of Fig. 13 shows the trend in drag coefficient with nacelle exit span location at both the leading edge and 1 exit-diam aft of the leading edge for configurations with the exits 1 exit-diam above the wing. As mentioned in the previous discussion, the trend is for the wing-body drag coefficient to be reduced as the nacelles are moved outboard. The second part of Fig. 13 presents the trends in drag coefficient with longitudinal position relative to the wing leading edge and with vertical position above the wing both at the 25% semispan station. Again, the 1½ exit-

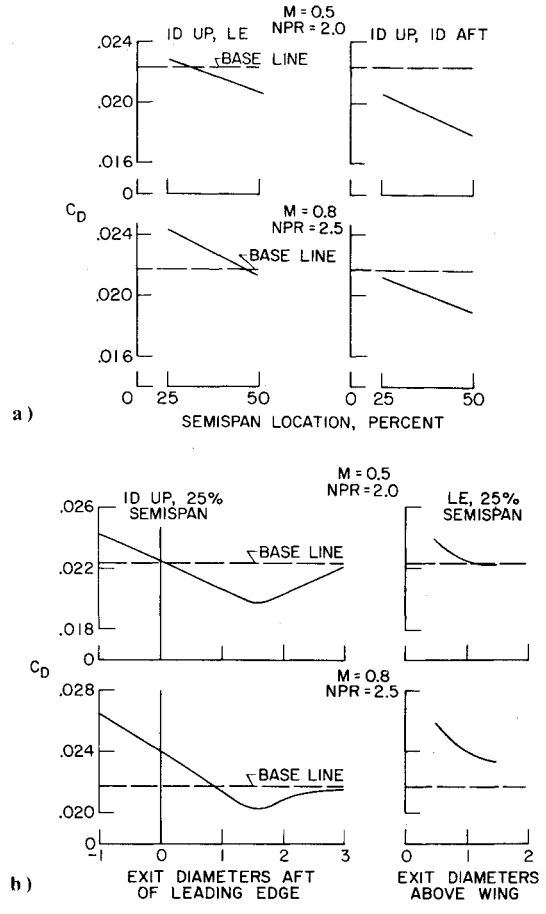

Fig. 13 Effect of nacelle exit location on wing-body drag at $C_L = 0.3$. a) Effect of semispan location; b) Effect of longitudinal and vertical location.

diam aft of the leading-edge configuration has the lowest drag for this lift coefficient of all longitudinal positions tested. As far as vertical location is concerned, the 1½ exit-diam above the wing configuration has the lowest drag of this series. Unfortunately, no positions above the 1½ exit-diam above the wing were tested, but the shape of the curves at both $M = 0.5$ and 0.8 possibly indicate that the minimum drag coefficient has been reached. Also indicated on the figure is the drag of the baseline wing-body configuration at $C_L = 0.3$ and, as can be seen, there are several configurations with jets operating which yield lower drag than the baseline. This result is extremely encouraging and adds impetus to the need for further exploration of over-the-wing pylon-mounted nacelles. Tests with a model having metric pylons and nacelles are especially needed.

Concluding Remarks

The current investigation of the effect of over-the-wing nacelles on wing-body aerodynamic characteristics has indicated a number of significant results. Jet operation has a detrimental effect on wing-body drag (when compared with jet-off drag) for this type of configuration arrangement. Most of this adverse effect occurs when the jet is initially turned on with virtually no further change in drag coefficient until the jet total pressure ratio reaches 3 and above. However, the interference on the wing-body due to the presence of the nacelles is beneficial, such that in some cases the drag of the wing-body with nacelles and jets operating is lower than that of the baseline wing-body. (It should be noted that the nacelles were not metric and as such it was impossible to ascertain the effects on them.) Of the configurations investigated, the one with the lowest drag has the nacelles installed 1 nacelle exit-diam above the wing, 1 nacelle exit-diam

aft of the leading edge, at the 50% semispan station. Unfortunately, due to one-engine-out controllability considerations, this configuration would probably not be acceptable for a twin-engine configuration such as that investigated. Of the configurations investigated at the 25% semispan station, the configuration with the nacelle exits 1 nacelle exit-diam above the wing and 1½ nacelle exit-diam aft of the leading edge has the lowest drag in the range of typical cruise-lift coefficients. Concurrent with the beneficial effects on wing-body drag, the effect of the nacelles on the wing-body lift are generally small and beneficial when compared to the lift of the baseline wing-body. The effects of the nacelles on wing-body pitching moment are also generally small. These last two results are encouraging in that the drag benefits from this type of configuration arrangement may be accrued without any extreme trim drag penalties.

References

[1] Falk, H., "The Influence of the Jet of a Propulsion Unit on Nearby Wings," TM 1104, NACA, 1946.

[2] Putnam, L.E., "Exploratory Investigation at Mach Numbers From 0.40 to 0.95 of the Effects of Jets Blown Over a Wing," TN D-7367, NASA, 1973.

[3] Krenz, G. and Ewald, B., "Airframe-Engine Interaction for Engine Configurations Mounted Above the Wing; Part I: Interference Between Wing and Intake/Jet; Part II: Engine Jet Simulation Problems in Wind Tunnel Tests," Paper 26, CP 150, AGARD, 1975.

[4] Mercer, C.E. and Carson, G.T., Jr., "Upper Surface Nacelle Influence on SCAR Aerodynamic Characteristics at Transonic Speeds," Paper 7, CP-001, NASA, 1976.

[5] Coe, P.L., Jr., McLemore, H.C., and Shivers, J.P., "Effects of Upper-Surface Blowing and Thrust Vectoring on Low-Speed Aerodynamic Characteristics of a Large-Scale Supersonic Transport Model," TN D-8296, NASA, 1976.

[6] Putnam, L.E., "An Analytical Study of the Effects of Jets Located More Than One Jet Diameter Above a Wing at Subsonic Speeds," TN D-7754, NASA, 1974.

[7] Ahmed, S.R., "Prediction of the Optimum Location of a Nacelle Shaped Body on the Wing of a Wing-Body Configuration by Inviscid Flow Analysis," Paper 25, CP 150, AGARD, 1975.

[8] Lan, C.E. and Campbell, J.F., "Theoretical Prediction of Jet Interaction Effects for USB and OWB Configurations," Paper 13, SP-406, NASA, 1976.

[9] Lan, C.E., Fillman, G.L., and Fox Jr., C.J., "Computer Program for Calculating Aerodynamic Characteristics of Upper-Surface-Blowing and Over-Wing-Blowing Configurations," TM X-73987, NASA, 1977.

[10] Lan, C.E., Campbell, J.F., and Fillman, G.L., "Theoretical Prediction of Over Wing Blowing Aerodynamics," presented as Paper 77-575 at the AIAA/NASA Ames V/STOL Conference, Palo Alto, Calif., June 6-8, 1977.

[11] Reubush, D.E., "An Investigation of Induced Drag Reduction Through Over-the-Wing Blowing," presented as Paper 77-884 at the AIAA/SAE 13th Joint Propulsion Conference, Orlando, Fla., July 11-13, 1977.

[12] Braslow, A.L. and Knox, E.C., "Simplified Method for Determination of Critical Height of Distributed Roughness Particles for Boundary-Layer Transition at Mach Numbers From 0 to 5," TN 4363, NACA, 1958.

[13] Braslow, A.L., Hicks, R.M., and Harris Jr., R.V., "Use of Grit-Type Boundary-Layer-Transition Trips on Wind Tunnel Models," TN D-3579, NASA, 1966.